



HAL
open science

Analysis of nanoindentation tests in SiC-based ceramics

Stefano Guicciardi, Cesare Melandri, Diletta Sciti, Giuseppe Pezzotti

► **To cite this version:**

Stefano Guicciardi, Cesare Melandri, Diletta Sciti, Giuseppe Pezzotti. Analysis of nanoindentation tests in SiC-based ceramics. *Philosophical Magazine*, 2006, 86 (33-35), pp.5321-5329. 10.1080/14786430600681639 . hal-00513691

HAL Id: hal-00513691

<https://hal.science/hal-00513691>

Submitted on 1 Sep 2010

HAL is a multi-disciplinary open access archive for the deposit and dissemination of scientific research documents, whether they are published or not. The documents may come from teaching and research institutions in France or abroad, or from public or private research centers.

L'archive ouverte pluridisciplinaire **HAL**, est destinée au dépôt et à la diffusion de documents scientifiques de niveau recherche, publiés ou non, émanant des établissements d'enseignement et de recherche français ou étrangers, des laboratoires publics ou privés.



Analysis of nanoindentation tests in SiC-based ceramics

Journal:	<i>Philosophical Magazine & Philosophical Magazine Letters</i>
Manuscript ID:	TPHM-05-Oct-0446.R2
Journal Selection:	Philosophical Magazine
Date Submitted by the Author:	28-Feb-2006
Complete List of Authors:	Guicciardi, Stefano; National Research Council, Institute of Science and Technology for Ceramics Melandri, Cesare; National Research Council, Institute of Science and Technology for Ceramics Sciti, Diletta; National Research Council, Institute of Science and Technology for Ceramics Pezzotti, Giuseppe; Kyoto Institute of Technology, Ceramic Physics Laboratory
Keywords:	silicon carbide, hardness, nanoindentation
Keywords (user supplied):	young



Analysis of nanoindentation tests in SiC-based ceramics

S. GUICCIARDI,^{1,2} C. MELANDRI,¹ D. SCITI,^{1,2} and G. PEZZOTTI^{2,3}

¹Institute of Science and Technology for Ceramics - National Research Council, via Granarolo 64, I-48018 Faenza, Italy

²RIN, Research Institute for Nanoscience, Kyoto Institute of Technology, Sakyo-ku, Matsugasaki, 606-8585 Kyoto, Japan

³Department of Chemistry and Materials Technology, Kyoto Institute of Technology, Sakyo-ku, Matsugasaki, 606-8585 Kyoto, Japan

Abstract

Two silicon carbide-based ceramics, with very different mean grain size, and a standard fused silica sample were characterized by nanoindentation. The values of hardness and Young's modulus were measured at several peak loads and calculated using the models developed by Oliver and Pharr (O&P) and by Cheng et al. (C&C). For all the materials, the values of hardness and Young's modulus were strongly dependent on the adopted model. In the silica specimen, the C&C Young's modulus and hardness were lower than those calculated by the O&P model. In the SiC ceramics, the differences between the two models were both qualitative and quantitative. The C&C Young's modulus values were lower than those calculated by the O&P model but the hardness values were higher. For most of the peak loads, the O&P model distinguished between the two SiC specimens while the C&C model did not.

Key words: nanoindentation, silicon carbide, hardness, Young's modulus

1. Introduction

Depth-sensing indentation (DSI) test is a unique technique in order to test materials down to microstructural level. However, the reliability of the results can be heavily affected by experimental issues. In the model developed by Oliver and Pharr (O&P) [1], the most used model for calculating the value of Young's modulus and hardness from loading-unloading curves, the area function of the indenter has to be precisely calibrated. This is usually done on a standard material like fused silica. However, there are situations in which the contact area between the material and indenter largely deviates from the area function calculated according to the displacement [2]. This happens when the indented material shows pileup of the displaced material around the indentation. Recently, based on dimensional analysis and finite elements calculations, Cheng et al., in the following indicated as C&C, developed an alternative model to derive indentation hardness and Young's modulus from loading-unloading curves which avoids the problem to determine the area function of the indenter [3, 4]. According to these authors, their model should have some advantages over that of O&P [5]: some calculations are carried out considering the whole loading-unloading curve, and not just a single

* Corresponding author: stefano@istec.cnr.it

point as in the O&P model, and, for not considering the contact area, the final results should not be affected by the eventual pile-up or sink-in around the indentation site.

In this work, DSI tests were carried on a standard fused silica specimen and two silicon carbide (SiC) specimens in a wide peak load range. The values of hardness and Young's were calculated according to the two models and compared. Hard structural ceramics like SiC are considered paradigm of materials for which the O&P model best applies [5]. As a such, they should allow the comparison of the two models more straightforwardly. The different mean grain size of the SiC ceramics should also indicate the influence of the microstructural scale length on the calculated properties.

2. Materials and testing

As testing materials a standard fused silica specimen and two different SiC ceramics were considered. The SiC ceramics were sintered by hot-pressing using yttria and alumina as sintering aids. The microstructures of the sintered specimens are shown after plasma-etching in figure 1. The mean grain sizes were calculated as 540 and 78 nm, respectively, by image analysis. For identification purposes, the SiC specimens have been labelled using their mean grain size, i.e. S540 and S78. More details on processing and characteristics of the materials are reported in Ref. [6] for sample S540 and Ref. [7] for samples S78.

[Insert figure 1 about here]

The depth-sensing indentation tests were performed in a nanoindenter (Nano Indenter XP™, MTS Systems Corporation, Oak Ridge, TN, USA) with a diamond Berkovich indenter. The polished SiC specimens were glued to aluminium cylinders as it was the case for the standard fused silica specimen. Six peak loads were used to investigate the indentation hardness and Young's modulus as a function of penetration depth: 1, 10, 50, 100, 200 and 400 mN for the silica specimen and 5, 10, 50, 100, 200 and 400 mN for the SiC specimens. The indenter was continuously loaded with prescribed loading rate up to the peak load and immediately unloaded with no holding time. For each peak load, at least ten indentations, spaced at 50 μm, were made. Indentation hardness (H) and Young's modulus (E) were calculated on the raw load-displacement data using a commercial software (MATHEMATICA 5.0, Wolfram Inc., Chicago, IL, USA). The raw data had the machine compliance and the thermal drift automatically subtracted by the data acquisition software of the nanoindenter (TestWorks™ ver. 4.06A). H^{OP} and E^{OP} (in the following, OP superscript letters indicate the O&P model while CC stands for the C&C model) of the tested material were calculated from the loading-unloading curves of the load, P , as a function of the displacement, h :

$$H^{OP} = \frac{P_{\max}}{A_c} \quad (1)$$

$$E^{OP} = \frac{1 - \nu^2}{\frac{1}{E_r} - \frac{1 - \nu_i^2}{E_i}} \quad (2)$$

where P_{\max} is the peak load, A_c the contact area, and E^{OP} , E_r , ν , ν_i are the Young's modulus and the Poisson

ratio of the material and indenter ($E=1141$ GPa and $\nu=0.07$), respectively. E_r , the reduced Young's modulus, is calculated from the unloading data as

$$E_r = \frac{\sqrt{\pi}}{2} S \frac{1}{\beta \sqrt{A_c}} \quad (3)$$

where β is a constant equal to 1.034 for a berkovich indenter and S is the contact stiffness. The contact stiffness is calculated by fitting a percentage, 90% in our case, of the unloading data by a polynomial function $b(h-h_0)^m$ and then taking the derivative of this function with respect to the displacement, i.e. dP/dh , and numerically evaluate it at the beginning of the unloading curve. In the O&P model, the contact area, A_c ,

is defined by a polynomial function $\left(A_c = \sum_{n=0}^8 C_n h_c^{2-n} \right)$ of the contact depth, h_c , which is given by

$$h_c = h_{\max} - \varepsilon \frac{P_{\max}}{S} \quad (4)$$

where h_{\max} is the displacement at the maximum load. ε was not taken as a constant equal to 0.75 but calculated according to [8]:

$$\varepsilon = m \left[1 - \frac{2(m-1)\Gamma\left(\frac{m}{2(m-1)}\right)}{\sqrt{\pi}\Gamma\left(\frac{1}{2(m-1)}\right)} \right] \quad (5)$$

where m is the fitted exponent of the unloading polynomial and Γ is the gamma function. The coefficients C_i of the area function were determined by a least-squares procedure on indentation tests carried out at different peak loads on the standard silica specimen. For the silica specimen, a Poisson ratio of 0.17 was used. The best result, i.e. the minimum difference with respect to the reference value of 72 GPa, was obtained with an area function described by four coefficients with values $C_0 = 24.056118$, $C_1 = 462.056784$, $C_2 = 18.748489$ and $C_3 = 715.770384$.

According to the C&C model, the indentation hardness (H^{CC}) and Young's modulus (E^{CC}) of a material can be calculated by the following equations [3, 4]:

$$\frac{H^{CC}}{E_r} = \frac{1}{\lambda(1+\gamma)} \frac{W_{unl}}{W_{tot}} \quad (6)$$

$$\frac{H^{CC}}{E_r^2} = \frac{4}{\pi} \frac{P_{\max}}{S^2}, \quad (7)$$

1
2
3 where $\lambda=0.27$ and $\gamma=1.5 \tan \theta + 0.327$, respectively. θ is the semi-angle of the cone with an equivalent
4 (area/penetration depth) of the berkovich indenter and can be estimated by the first coefficient of the area
5 function, C_0 . W_{tot} and W_{unl} are the areas under the loading and unloading curves, respectively. The other
6 symbols have the same meaning as above. The numerical integration of the loading and unloading curves
7 was carried out using the mathematical software already indicated. For all the SiC materials, a Poisson's
8 ratio of 0.19 was used [9].
9
10

11 3. Results

12
13
14 The silica Young's modulus and hardness calculated according to the two models are shown in figure 2. As
15 can be seen, the O&P Young's modulus and hardness were higher than the corresponding C&C properties.
16 For both models, the calculated properties were almost load-independent. The O&P Young's modulus very
17 nicely agree with the reference value of 72 GPa. The O&P hardness is in better agreement than the C&C
18 hardness with other published results [10-12], even without a reference value to be compared to.
19
20

21 [Insert figure 2 about here]
22
23

24 The Young's modulus and hardness of the two SiC specimens are shown in figure 3 as a function of
25 peak load and tested material. The trend of the Young's modulus with the peak load was almost independent
26 on the adopted model: non-monotonous for the S540 specimen (this phenomenon was more evident for the
27 O&P model) and practically constant for the S78 specimen. The O&P Young's modulus values were higher
28 than those calculated according to the C&C model for both the SiC specimens. For most of the peak loads,
29 the O&P Young's modulus was different for the two SiC specimens. This difference was not observed for the
30 C&C values, see figure 3a.
31
32

33 [Insert figure 3 about here]
34
35

36 At the highest peak loads, the C&C hardness values were higher than the O&P values for both the
37 SiC specimens, see figure 3b. With the C&C model, no difference was observed between the two SiC
38 specimens whose values were almost load independent. On the other hand, with the O&P model, the two
39 SiC specimens showed a very different behaviour. While the hardness of specimen S78 was almost load-
40 independent, the hardness of S540 decreased by increasing the peak load so that, at the highest peak
41 loads, the O&P hardness of the two SiC specimens converged. At the lowest peak loads, the O&P hardness
42 of specimen S540 was about the same as the C&C hardness.
43
44

45 4. Discussion

46
47
48 In the O&P model, one of the main concern is that the estimated contact area coincides with the real contact
49 area. An indirect indication of this circumstance is that the ratio h/h_{max} is <0.7 [2]. The value of this ratio is
50 shown in figure 4 for the tested materials as a function of the peak load. All the values are well below 0.7.
51
52
53
54
55
56
57
58
59
60

1
2 AFM analysis of nanoindentations in a fused silica specimen experimentally confirmed that this material
3 shows no pileup [13]. However, in the same paper, some pileup was observed around the nanoindentations
4 in a structural ceramics such as Si_3N_4 for which the ratio h_f/h_{max} is typically <0.7 [14]. The eventual presence
5 of pileup around nanoindentations in our SiC specimens could have therefore slightly overestimated our O&P
6 values.
7

8
9 [Insert figure 4 about here]

10
11 In the fused silica specimen, where the O&P results were not affected by pileup, the expected
12 agreement between the experimental values of O&P Young's modulus and the reference value of 72 GPa
13 indicates that the tip area function was properly calibrated and, at the same time, that the frame compliance
14 and the thermal drift were correctly subtracted from the raw load-displacement data. Using the C&C model,
15 the Young's modulus and hardness of the fused silica specimen turned out to be load-independent as those
16 calculated using the model of O&P. However, the C&C values of Young's modulus and hardness do not well
17 compare with published results. In our case, the numerical differences were about 14% and 25% for Young's
18 modulus and hardness, respectively, and the reasons for such a discrepancy are not clear at the moment.
19

20
21 Also for the SiC specimens, the differences between the O&P model and the C&C model were
22 quantitative. As a possible explanation for the numerical discrepancy, we can point out that some of the
23 relationships involved in the C&C model do not seem to hold in our case. For example, a linear relationship
24 between $(W_{\text{tot}}-W_{\text{unl}})/W_{\text{tot}}$ and h_f/h_{max} proposed in [4] as:
25

$$\frac{W_{\text{tot}} - W_{\text{unl}}}{W_{\text{tot}}} = (1 + \lambda) \frac{h_f}{h_{\text{max}}} - \lambda \quad (8)$$

26
27
28 with $\lambda=0.27$ was not confirmed on our experimental data, see figure 5. It is however fair to remember that the
29 finite-element simulation presented in [4] encompassed a very large range for h_f/h_{max} , between 0.3 and 1,
30 whereas in our case this range was much smaller, see figure 5.
31

32
33 Using the two models, a further difference emerged. The O&P model seems to differentiate the
34 Young's modulus and the hardness of the two SiC specimens for most of the peak loads used but the C&C
35 model gave results very often undistinguishable. The difference in the O&P results between the two SiC
36 specimens was previously attributed to the influence of the different mean grain size on the properties of the
37 materials [15]. Being the nanoindentation tests performed at the same scale length of the microstructure, an
38 influence of the grain size on the measured mechanical properties should be expected, in particular for
39 hardness as many experimental results indicate [16, 17]. This was not the case with the C&C results which
40 apparently ignore the effects of the microstructure on the calculated properties.
41
42
43
44

45
46 [Insert figure 5 about here]

47
48 No other experimental works on monolithic ceramics are known to the authors. The only other
49 comparison is on carbon nitride films [18, 19]. In those papers, the Young's modulus calculated by the two
50 methods were not very different, but the hardness calculated by C&C was higher. The main difference with
51

our analysis is that area function of the Berkovich indenter was there taken with the leading term C_0 equal to 24.5, i.e. a perfect shape, while it has been shown that in order to get the best possible area function calibration this condition has to be relaxed [20]. The leading term C_0 influences also the term depending on θ in eq. (6).

Formatted: Font: Italic

Formatted: Font: Italic, Subscript

Formatted: Font: Italic

Formatted: Font: Italic, Subscript

Deleted: Due to the lack of other experimental works using the C&C model, there is no the possibility to compare our results with similar investigations.

A final remark on the applicability of the C&C model on advanced ceramics such as those used for this work. The C&C model was based on finite element simulation considering continuum mechanics and Mises effective stress which very well fit metals plasticity. Even if C&C themselves compared their model forecasts with experimental results on ceramics and silica [3, 4], it could be that these conditions are not generally met in case of advanced polycrystalline ceramics due to a different plastic flow rule or to the influence of the microstructure [21]. From this point of view, we cannot generalize our conclusions. However, for the specific SiC ceramics, in a finite element simulation which considered a pressure sensitive flow rule, it was shown that experimental results on SiC were in very good agreement with the classic plasticity based on Mises effective stress [21].

Deleted: [Insert figure 5 about here]

5. Conclusions

Nanoindentation tests were carried out at different peak load in a standard fused silica specimen and two silicon carbide ceramics with very different mean grain size. The Young's modulus and the hardness were calculated using the models developed by Oliver and Pharr (O&P) and by Cheng et al. (C&C). The results were different both qualitatively and quantitatively. In particular, on the silica specimen, the C&C Young's modulus and hardness were lower than the corresponding O&P values. For both models, the silica properties were load-independent. In the SiC specimens, the C&C Young's modulus was lower than the O&P values, but the opposite was true for the hardness. Especially for hardness, the load dependence was also different in the two models. For most of the peak loads used, the O&P properties were generally different in the two SiC specimens, while with the C&C model such a difference was not observed. Some intermediate experimental results seems to be different from the theoretical predictions of the C&C model. The influence of the microstructure on indentation results, which is not considered in the C&C model, could be higher than expected.

References

- [1] W. C. Oliver and G. M. Pharr, *J. Mater. Res.* **7** 1564 (1992).
- [2] A. Bolshakov and G. M. Pharr, *J. Mater. Res.* **13** 1049 (1998).
- [3] Y.-T. Cheng and C.-M. Cheng, *Appl. Phys. Lett.* **73** 614 (1998).
- [4] Y.-T. Cheng, Z. Li Z. and C.-M. Cheng, *Phil. Mag. A* **10** 1821 (2002).
- [5] Y.-T. Cheng and C.-M. Cheng, *Mater. Sci. Eng. R* **44** 91 (2004).
- [6] D. Sciti and A. Bellosi, *J. Mater. Sci.* **35** 3849 (2000).
- [7] D. Sciti, J. Vicens, N. Herlin, J. Grabis and A. Bellosi, *J. Ceram. Proc. Res.* **5** 40 (2004).
- [8] G. M. Pharr, A. Bolshakov, *J. Mater. Res.* **17** 2660 (2002).
- [9] CRC Materials Science and Engineering Handbook, J. F. Shackelford, W. Alexander, Eds., CRC Press, USA, 2001.
- [10] J. A. Knapp, D. M. Follstaedt, S. M. Meyers, J. C. Barbour and T. A. Friedman, *J. Appl. Phys.* **85** 1460 (1999).
- [11] K. Ikezawa and T. Tadashi, *J. Appl. Phys.* **91** 9689 (2002).
- [12] Y. W. Bao, W. Wang, Y. C. Zhou, *Acta Mater.* **52** 5397 (2004).
- [13] M. Suganuma, M. V. Swain, *J. Mater. Res.* **19** 3490 (2004).
- [14] J. Gong, H. Miao, Z. Peng and L. Qi, *Mater. Sci. Eng. A* **354** 140 (2003).
- [15] S. Guicciardi, D. Sciti, C. Melandri and A. Bellosi, *J. Am. Ceram. Soc.* **87** 2101 (2004).
- [16] I. J. McColm, *Ceramic Hardness* (Plenum Press, New York, 1990).
- [17] R. W. Rice, C. Cm. Wu and F. Boichelt, *J. Am. Ceram. Soc.*, **77** 2539 (1994).
- [18] Y. Kusano, I. M. Hutchings, *Surf. Coat. Techn.* **169-170** 739 (2003).
- [19] Y. Kusano, Z. H. Barber, J. E. Evetts, I. M. Hutchings, *Surf. Coat. Techn.* **174-175** 601 (2003).

Formatted: English (U.K.)

Formatted: Font: Bold

Formatted: English (U.K.)

1
2
3 [20] W. C. Oliver, G. M. Pharr, J. Mater. Res., 19 3 (2004).

Formatted: Font: Bold

4
5
6 [21] A. E. Giannakopoulos, P.-L. Larsson, Mechanics of Materials, 25 1 (1997).

Formatted: Font: Bold

7
8
9
10
11
12
13
14
15
16
17
18
19
20
21
22
23
24
25
26
27
28
29
30
31
32
33
34
35
36
37
38
39
40
41
42
43
44
45
46
47
48
49
50
51
52
53
54
55
56
57
58
59
60

For Peer Review Only

Figure captions

- 1
2
3
4
5
6 Figure 1. SEM micrograph of the plasma-etched surfaces of SiC specimens showing the microstructure:
7 (a) nano-sized SiC, mean grain size 78 nm; (b) micro-sized SiC specimen, mean grain size
8 540 nm. Around the SiC grains (gray areas) boundaries, the intergranular phase is visible. Due
9 to the plasma-etching technique, its volumetric fraction is overestimated on the micrograph.
10
11 Figure 2. Plot of the Young' modulus (a) and hardness (b) of the silica specimen as a function of the
12 peak load calculated according to the models of Oliver and Pharr (O&P) and Cheng and
13 Cheng (C&C). Points and bars represent mean±1 standard deviation, respectively. In the
14 Young's modulus plot, the solid line indicates the reference value of 72 GPa.
15
16
17 Figure 3. Plot of the Young' modulus (a) and hardness (b) of the two SiC specimens as a function of the
18 peak load calculated according to the models of Oliver and Pharr (O&P) and Cheng and
19 Cheng (C&C). Points and bars represent mean±1 standard deviation, respectively. The points
20 have been slightly shifted for a better readability.
21
22
23 Figure 4. Plot of the ratio h_f/h_{max} as a function of peak load and material. Points and bars represent
24 mean±1 standard deviation, respectively.
25
26
27 Figure 5. Regression plot of $(W_{tot}-W_{uni})/W_{tot}$ versus the ratio h_f/h_{max} for the three tested materials. Points
28 and bars represent mean±1 standard deviation, respectively. The standard errors of the slope
29 and intercept are ±0.052 and ±0.027, respectively.
30
31
32
33
34
35
36
37
38
39
40
41
42
43
44
45
46
47
48
49
50
51
52
53
54
55
56
57
58
59
60

Figures

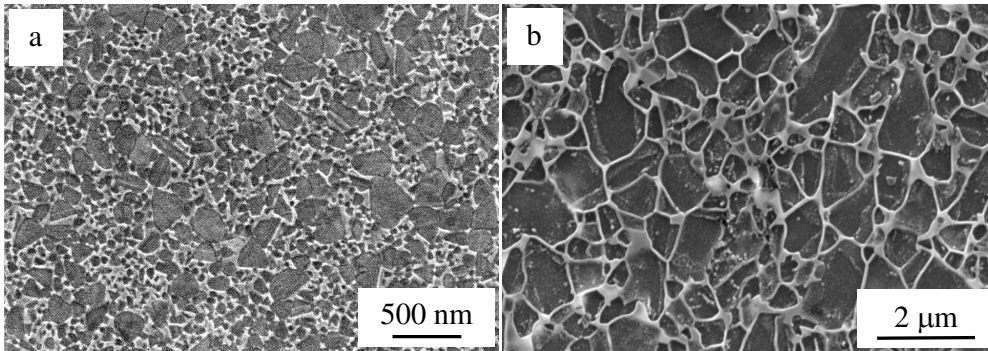


Figure 1

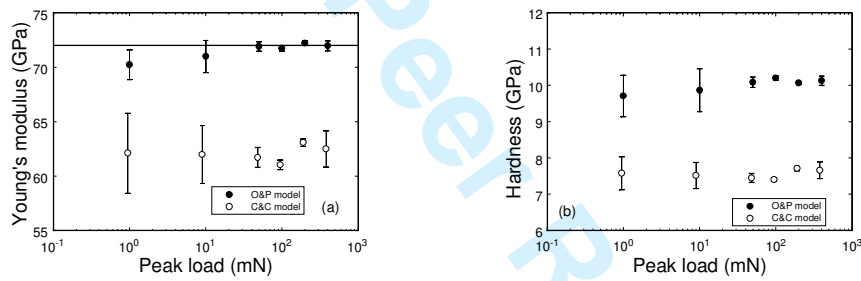


Figure 2

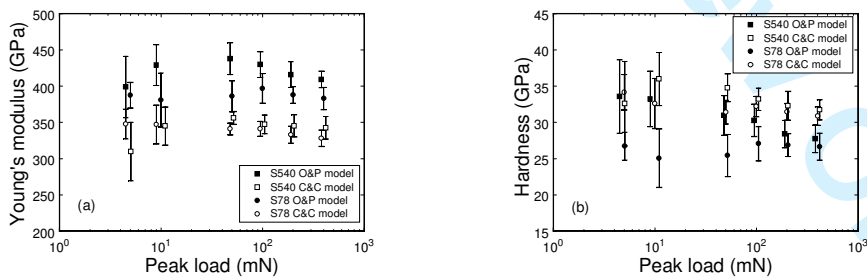


Figure 3

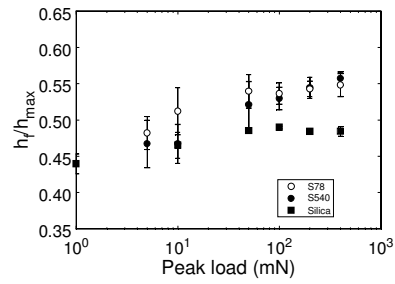


Figure 4

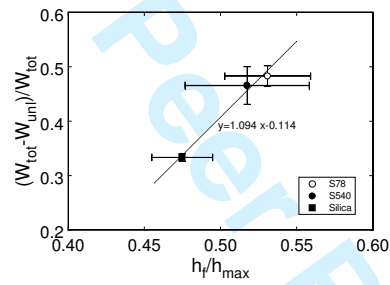


Figure 5